

# Sensitivity analysis of narrowband photonic crystal filters and waveguides to structure variations and inaccuracy

Ben Zion Steinberg, Amir Boag, and Ronen Lisitsin

Faculty of Engineering, Tel Aviv University, Ramat-Aviv, Tel-Aviv 69978, Israel

Received June 9, 2002; revised manuscript received August 16, 2002; accepted August 19, 2002

Photonic crystal microcavities, formed by local defects within an otherwise perfectly periodic structure, can be used as narrowband optical resonators and filters. The coupled-cavity waveguide (CCW) is a linear array of equally spaced identical microcavities. Tunneling of light between microcavities forms a guiding effect, with a central frequency and bandwidth controlled by the local defects' parameters and spacing, respectively. We employ cavity perturbation theory to investigate the sensitivity of microcavities and CCWs to random structure inaccuracies. For the microcavity, we predict a frequency shift that is due to random changes in the lattice structure and show an approximate linear dependence between the standard deviation of the structure inaccuracy and that of the resonant frequency. The effect of structural inaccuracy on the CCW devices, however, is different; it has practically no effect on the CCW performance if it is below a certain threshold but may destroy the CCW if this threshold is exceeded. © 2003 Optical Society of America

OCIS code: 130.2790.

## 1. INTRODUCTION

Photonic bandgap materials attracted much attention in the context of designing optical and microwave devices. Recently numerical experiments have shown that line defects in photonic crystals can be used not only to guide but also to multiplex and demultiplex optical signals.<sup>1</sup> Most researchers studying the waveguiding by line defects employ photonic waveguides obtained by removal of a contiguous line of posts in the periodic structure. In such a setting, the strong coupling between the adjacent defects produces relatively wideband waveguides.

In this paper we perform a sensitivity analysis of photonic crystal waveguides and filters with a prescribed center frequency and narrow bandwidth. Specifically, we concentrate on microcavities and on the coupled-cavity waveguide (CCW) configuration, proposed recently by a few researchers in different independent studies and for different applications<sup>2-6</sup> (in Ref. 6 the CCW was termed the microcavity array waveguide). In the CCW, a waveguide is formed by widely spaced periodic identical defects in the photonic crystal. Each defect site with a resonant frequency in the bandgap serves as a microcavity. Tunneling of radiation between the defect sites allows wave propagation along the line of defects. Sections of such waveguides can be employed as ultranarrow band filters in optical routing devices. A schematic description of the CCW is shown in Fig. 1.

In previous papers, these devices were studied by employing the weakly coupled cavity model. This approach resembles the tight-binding perturbation theory of solid-state physics.<sup>7</sup> It has been shown that the center frequency of the waveguide is determined mainly by the resonant frequency of the single defect, say  $\omega_0$ . Weak coupling between the periodic defects causes the discrete spectral line at  $\omega_0$  to turn into a narrow band of guided

frequencies only slightly shifted from the original frequency of a single defect. The resulting waveguide dispersion relation  $\omega(\beta)$  is

$$\omega - \omega_0 \approx \omega_s + \Delta\omega \cos \beta. \quad (1.1)$$

The perturbation theory facilitates an approximate calculation of both the frequency shift  $\omega_s$  and the half-frequency bandwidth of the periodic microcavity waveguide,  $\Delta\omega$ . These parameters are linked by an analytic relationship to the distance vector between the defect sites  $\mathbf{b}$  (see Refs. 5 and 6). For example, it has been shown that  $\omega_s \ll \Delta\omega$  and the bandwidth  $\Delta\omega$  decreases exponentially with  $\mathbf{b}$ . Thus, by tuning the distance between the defect sites, one can achieve extremely narrowband filters and optical routers,<sup>6</sup> and, by a proper design and control of the local defect, one can obtain almost any prescribed central frequency  $\omega_0$ .

As a result of the above-mentioned appealing properties, effort has been devoted to use these devices in optical communication applications in which the operating wavelengths are in the 1.5- $\mu\text{m}$  regime. Thus structural details of photonic crystal devices designed to operate in the optical regime may have sizes in the deep submicrometer scale, which evidently approaches the accuracy limits of conventional fabrication technologies.

The purpose of this paper is to examine sensitivity aspects related to the microcavity resonance frequency  $\omega_0$  and their ramifications on the CCW filter design. More specifically, three goals are addressed:

1. Extension of the cavity perturbation theory,<sup>8</sup> traditionally employed for microwave cavity tuning analysis, to study the shift of an isolated microcavity frequency  $\omega_0$  as a function of the local defects' parameters.

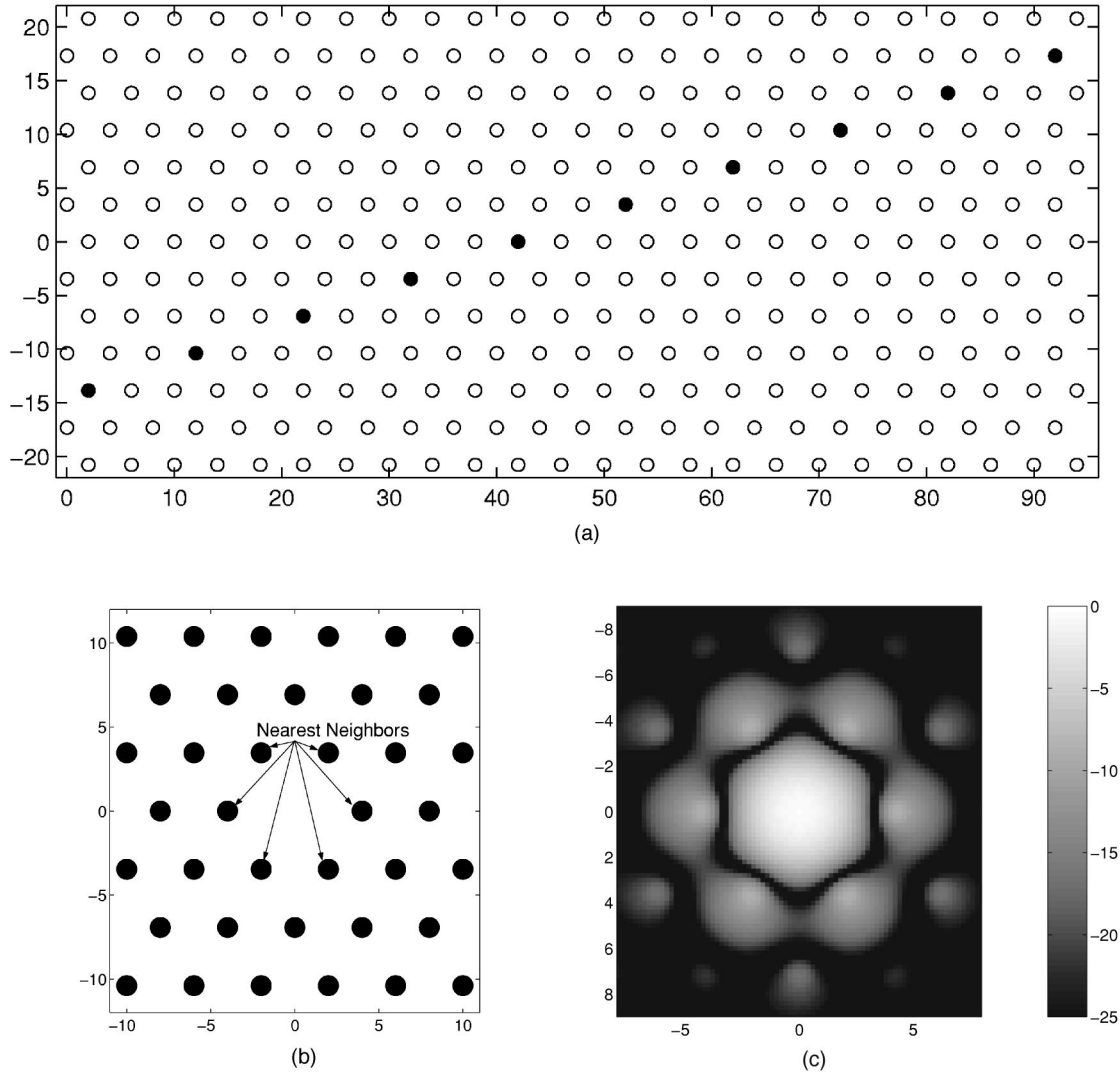


Fig. 1. CCW (or array waveguide) and its components. (a) Schematic description of the CCW in an otherwise perfect 2D hexagonal crystal. Solid circles, microcavities created by local defects. The intercavity distance is  $b$ . (b) Example of a local defect microcavity, created by removing a single post. (c) Isolated microcavity modal field  $E_0$ .

2. Use of the above theory to investigate the influence of random structure inaccuracies on the single cavity center frequency, and comparison of its results to exact computations.

3. Study of the CCW sensitivity to random structure inaccuracies. This study is based on the fact that the microcavities are weakly coupled; hence the entire CCW can be viewed as a linear array of microcavities having independent random resonant frequencies.

Throughout this study the analytically derived theoretical results are supported by numerical computations that demonstrate their efficacy and range of validity. Our numerical test problem is based on the hexagonal-lattice structure studied in a previous publication of the authors.<sup>6</sup> The selected photonic bandgap structure possesses a bandgap for wavelengths between 7.5 and 10.5 in arbitrary length units, yielding a relative bandwidth of approximately 34%. This very large gap allows a study of the validity of our structure perturbation theory over a wider range of wavelengths and perturbation parameters.

## 2. EIGENVALUE VARIATION AND CAVITY PERTURBATION THEORY

The propagation of a time-harmonic electromagnetic wave in an inhomogeneous dielectric is governed by the following wave equation for the vector magnetic field  $H$ <sup>9</sup>:

$$\Theta H(r) = \lambda H(r), \quad \lambda = \left(\frac{\omega}{c}\right)^2, \quad (2.1)$$

where  $\omega$  is the frequency,  $c$  is the free-space speed of light, and  $\Theta$  denotes a self-adjoint operator defined by

$$\Theta H \equiv \nabla \times \left[ \frac{1}{\epsilon_r(r)} \nabla \times H \right]. \quad (2.1a)$$

Here  $\epsilon_r(r)$  is the relative dielectric property of the medium. When perfect or imperfect photonic crystal structures are considered, the above equation constitutes an eigenvalue problem that governs the electromagnetic modal field, where  $\lambda$  is an eigenvalue that determines the

structure resonances.<sup>9</sup> Specifically, we consider here the case in which  $\epsilon_r$  describes a photonic crystal with a single localized defect creating a microcavity with localized modal fields and corresponding eigenvalues.

### A. Nondegenerate Case

Here we assume that to each eigenvalue (resonance)  $\lambda_n$  of Eq. (2.1) corresponds only a single distinct modal field  $H_n$ . The main concern of the present study is to explore how the resonance changes as the dielectric structure is varied. Thus let the sets  $\{E_n(r)\}_{n=0,1,\dots}$  and  $\{H_n(r)\}_{n=0,1,\dots}$  be the electric and magnetic modal fields of a given photonic crystal structure  $\epsilon_r(r)$ , with the corresponding set of eigenvalues  $\{\lambda_n\}$ . Similarly, let the sets  $\{E_m^*(r)\}$ ,  $\{H_m^*(r)\}$ , and  $\{\lambda_m^*\}$  be those associated with a varied structure  $\epsilon_r^*(r)$ . We have

$$\Theta H_n(r) = \lambda_n H_n(r), \quad (2.2a)$$

$$\Theta^* H_m^*(r) = \lambda_m^* H_m^*(r), \quad (2.2b)$$

where  $\Theta^*$  is the operator defined in Eq. (2.1a) but associated with the varied structure  $\epsilon_r^*(r)$ . It should be emphasized that the modal fields are distinguished from the actual physical fields by their normalization,

$$H_n \equiv \mathcal{H}_n \left( \int |\mathcal{H}_n|^2 d^3r \right)^{-1/2}, \quad (2.3a)$$

$$E_n \equiv \mathcal{E}_n \left( \int |\mathcal{E}_n|^2 d^3r \right)^{-1/2}, \quad (2.3b)$$

where  $\mathcal{E}_n$ ,  $\mathcal{H}_n$  are the actual physical electric and magnetic modes in the photonic crystal microcavity [clearly, they satisfy Eq. (2.2a)]. With this normalization, the modal fields  $E_n$  and  $H_n$  possess the physical units of ohm  $\times$  meter<sup>-3/2</sup> and meter<sup>-3/2</sup>, respectively. Similar relations hold for the asterisked quantities. Since the modes are nondegenerate, we assume the eigenvalues are ordered such that

$$\lambda_n \neq \lambda_m^* \forall m \neq n. \quad (2.4)$$

Since the operator  $\Theta$  ( $\Theta^*$ ) is self-adjoint, the set  $\{H_n(r)\}$  ( $\{H_m^*(r)\}$ ) is complete and orthonormal in  $L_2$ . Note, however, that the electric field modes  $\{E_n(r)\}$  ( $\{E_m^*(r)\}$ ) are orthonormal with respect to a weight function  $\epsilon_r/\eta_0^2$  ( $\epsilon_r^*/\eta_0^2$ ). Thus

$$\langle H_n, H_m \rangle \equiv \int H_n \cdot \overline{H_m} d^3r = \delta_{mn}, \quad (2.5a)$$

$$\langle E_n \epsilon_r/\eta_0^2, E_m \rangle \equiv \int (\epsilon_r/\eta_0^2) E_n \cdot \overline{E_m} d^3r = \delta_{mn}, \quad (2.5b)$$

where the overbar denotes the complex conjugate. The corresponding norm in  $L_2$  is naturally defined via the inner product in Eq. (2.5a), as  $\|F\|^2 \equiv \langle F, F \rangle$ . It should be emphasized that the normalization in Eqs. (2.3a) and (2.3b) renders dimensionless the inner products in Eqs. (2.5a) and (2.5b) and the corresponding norm. Similar expressions hold for the asterisked quantities. Performing inner products of Eq. (2.2a) with  $H_m^*(r)$  and Eq. (2.2b) with  $H_n(r)$ , subtracting the resulting equations, performing integration by parts, and using the fact that  $\nabla \times H_n = -i\omega_n \epsilon E_n$ , we get

$$\begin{aligned} \omega_n \omega_m^* \langle \epsilon^* E_m^*, \epsilon_0 E_n \rangle - \omega_n \omega_m^* \langle \epsilon E_n, \epsilon_0 E_m^* \rangle \\ = \langle H_n, H_m^* \rangle (\lambda_n - \lambda_m^*). \end{aligned} \quad (2.6)$$

By realness of the eigenvalues and eigenfunctions ( $\Theta$  is self-adjoint), Eq. (2.6) can be rewritten as

$$\frac{\lambda_m^* - \lambda_n}{\epsilon_0^2 \omega_n \omega_m^*} \langle H_n, H_m^* \rangle = \langle E_n, \delta \epsilon_r E_m^* \rangle = \langle \delta \epsilon_r E_n, E_m^* \rangle, \quad (2.7)$$

where  $\delta \epsilon_r = \epsilon_r - \epsilon_r^*$ . From Eq. (2.7) we have

$$\begin{aligned} \sum_{m,m \neq n} |\langle H_n, H_m^* \rangle|^2 \\ = \eta_0^{-4} \sum_{m,m \neq n} \left| \frac{\omega_n \omega_m^*}{\omega_m^{*2} - \omega_n^2} \right|^2 |\langle (\delta \epsilon_r/\epsilon_r^*) E_n, \epsilon_r^* E_m^* \rangle|^2 \\ \leq \alpha_n^2 \sum_m |\langle (\delta \epsilon_r/\epsilon_r^*) E_n, (\epsilon_r^*/\eta_0^2) E_m^* \rangle|^2, \end{aligned} \quad (2.8)$$

where  $\alpha_n = \max_{m,m \neq n} |\omega_n \omega_m^*/(\omega_m^{*2} - \omega_n^2)|$  is finite owing to the fact that  $\omega_m^*$  increases with  $m$ . With the orthonormality relation in Eq. (2.5b), applied to the asterisked quantities, the squared elements within the rightmost sum can be viewed as the coefficients of a generalized Fourier expansion of  $(\delta \epsilon_r/\epsilon_r^*) E_n$  by the set  $\{E_m^*\}$ . Thus the sum is bounded by  $\eta_0^{-2} \|(\delta \epsilon_r/\sqrt{\epsilon_r^*}) E_n\|^2$  (apply Parseval's theorem with respect to a weighted inner product). This implies the following inequality:

$$\begin{aligned} \sum_{m,m \neq n} |\langle H_n, H_m^* \rangle|^2 &\leq \alpha_n^2 \eta_0^{-2} \|(\delta \epsilon_r/\sqrt{\epsilon_r^*}) E_n\|^2 \\ &\leq \alpha_n^2 \eta_0^{-2} \|\delta \epsilon_r/\sqrt{\epsilon_r^*}\|^2 \max_r |E_n|^2, \end{aligned} \quad (2.9)$$

which vanishes as  $\delta \epsilon_r \rightarrow 0$ . Note that both sides of this inequality are dimensionless (see Eqs. (2.3a) and (2.3b) and discussion thereafter).

It follows from inequality (2.9) that the eigenfunctions  $H_m^*$  dependence on  $\delta \epsilon_r$  is continuous, as shown by the following result (the proof is provided in the Appendix):

Let  $\{g_n^\delta\}$  be an orthonormal basis that depends on the parameter  $\delta$ . Let  $\{f_n\}$  be a sequence satisfying  $\|f_n\| = 1$ . If  $\sum_{m,m \neq n} |\langle f_n, g_m^\delta \rangle|^2 \rightarrow 0$  as  $\delta \rightarrow 0$ , then for any fixed  $n$ ,  $g_n^\delta \rightarrow f_n$  as  $\delta \rightarrow 0$ . Furthermore, if  $\sum_{m,m \neq n} |\langle f_n, g_m^\delta \rangle|^2 \leq O(\delta)$  as  $\delta \rightarrow 0$ , then for any fixed  $n$ ,  $\|g_n^\delta - f_n\| \leq O(\delta)$  as  $\delta \rightarrow 0$ .

Applying this result to Eq. (2.7) and relations (2.8) and (2.9) (that is,  $H_m^* \leftrightarrow g_m^\delta$ , and  $\delta \leftrightarrow \|\delta \epsilon_r/\epsilon_r^*\|$ ) in the limit of  $\delta \epsilon_r \rightarrow 0$  and using hypothesis (2.4), we get for all  $m$

$$\begin{aligned} H_m^* &= H_m + \delta H_m, \\ \|\delta H_m\| &\leq O(\|\delta \epsilon_r/\epsilon_r^*\|) \rightarrow 0 \quad \text{as } \|\delta \epsilon_r/\epsilon_r^*\| \rightarrow 0. \end{aligned} \quad (2.10)$$

Thus, for small perturbations in  $\epsilon_r$ , one can replace  $E_m^*$ ,  $H_m^*$  with  $E_m$ ,  $H_m$  in Eq. (2.7), since the contribution of  $\delta E$  and  $\delta H$  is second order owing to the multiplication with  $\delta \epsilon_r$ . (Note that the requirement for small  $\|\delta \epsilon_r/\epsilon_r^*\|$  does not impose small variations in  $\epsilon_r$  or low contrast; rather, the volume integration of the relative changes in

permittivity should be small.) Using this fact and applying Eq. (2.7) to the case  $m = n$ , we find  $[\lambda = (\omega/c)^2]$ :

$$\frac{\omega_n^{*2} - \omega_n^2}{\omega_n^* \omega_n} \approx \frac{\langle \mathbf{E}_n, \delta\epsilon_r \mathbf{E}_n \rangle}{\eta_0^2 \|\mathbf{H}_n\|^2}. \quad (2.11)$$

This last result describes the shift in the  $n$ th resonance frequency that is due to material variation  $\delta\epsilon_r$ . Finally, note that for small variations in  $\omega_n$  we can make the approximation  $\omega_n^{*2} - \omega_n^2 \approx 2\omega_n(\omega_n^* - \omega_n)$ . Thus

$$\delta\omega_n \approx \frac{\omega_n}{2} \frac{\langle \mathbf{E}_n, \delta\epsilon_r \mathbf{E}_n \rangle}{\eta_0^2 \|\mathbf{H}_n\|^2}, \quad (2.12)$$

where  $\delta\omega_n \equiv \omega_n^* - \omega_n$ .

### B. Degenerate Case

Owing to the highly symmetrical structure of photonic crystal microcavities, it often happens that for a perfect structure (i.e., in the absence of random structure inaccuracies), an eigenvalue  $\lambda_n$  is associated with  $N$  linearly independent modes  $\mathbf{H}_n^{(i)}$ ,  $i = 1, \dots, N$ —a situation referred to as  $N$ -fold degeneracy. In these cases, Eq. (2.2a) can take on a more general form,

$$\Theta \sum_{i=1}^N a_i \mathbf{H}_n^{(i)}(r) = \lambda_n \sum_{i=1}^N a_i \mathbf{H}_n^{(i)}(r), \quad (2.13)$$

where the coefficients  $\{a_i\}_{i=1, \dots, N}$  can be chosen arbitrarily. From the structure of Eq. (2.13), it is clear that any linear combination of degenerate modes is a degenerate mode, too. Specifically, one can exploit this fact and the linear independence of these modes to rebuild the set  $\mathbf{H}_n^{(i)}$ ,  $i = 1, \dots, N$  as an orthonormal set (say, via a Gram-Schmidt orthogonalization):

$$\langle \mathbf{H}_n^{(i)}, \mathbf{H}_n^{(j)} \rangle = \delta_{ij}, \quad i, j = 1 \dots N. \quad (2.13a)$$

Using Eq. (2.13) in conjunction with Eq. (2.2b) [instead of Eq. (2.2a)] and following the same steps that led to Eq. (2.7), we get

$$\sum_{i=1}^N a_i \langle \delta\epsilon_r \mathbf{E}_m^*, \mathbf{E}_n^{(i)} \rangle = \frac{\lambda_n - \lambda_m^*}{\epsilon_0^2 \omega_n \omega_m^*} \sum_{i=1}^N a_i \langle \mathbf{H}_n^{(i)}, \mathbf{H}_m^* \rangle. \quad (2.14)$$

We concentrate now on the new modes  $\mathbf{E}_m^*$ ,  $\mathbf{H}_m^*$  that result from the structure perturbation of the degenerate modal fields. Since those are expected to be close to each other, we assume that  $\mathbf{E}_m^*$  can be approximated by a sum of the degenerate modes and choose  $a_i$  to be the summation coefficients. Thus we have

$$\mathbf{E}_m^* = \sum_{j=1}^N a_j \mathbf{E}_n^{(j)}. \quad (2.15)$$

Substituting this expansion into Eq. (2.14), we get

$$\frac{\lambda_n - \lambda_m^*}{\epsilon_0^2 \omega_n \omega_m^*} = \frac{\sum_i \sum_j a_i \bar{a}_j \langle \delta\epsilon_r \mathbf{E}_n^{(j)}, \mathbf{E}_n^{(i)} \rangle}{\sum_i \sum_j a_i \bar{a}_j \langle \mathbf{H}_n^{(i)}, \mathbf{H}_n^{(j)} \rangle}. \quad (2.16)$$

The last result is an eigenvalue equation for the new  $\lambda_m^*$ , which possesses exactly the same structure as the eigenvalue problem studied in Ref. 6. It can be solved by looking for the stationary point of  $\lambda_m^*$  with respect to the co-

efficients  $a_i$ , using the very same procedure outlined in Ref. 6. Performing these steps and also using the orthonormality relation in Eq. (2.13a), we obtain the following matrix eigenvalue problem:

$$[\mathcal{A}][a] = \frac{\lambda_n - \lambda_m^*}{\epsilon_0^2 \omega_n \omega_m^*} [a], \quad (2.17)$$

which is written for the eigenvectors  $[a]$  (with elements  $a_i$ ), and the eigenvalues  $\lambda_m^*$ , for a given degenerate state  $(\lambda_n, \mathbf{E}_n^{(i)})_{i=1, \dots, N}$ . Here  $\mathcal{A}$  is an  $N \times N$  matrix with elements

$$\mathcal{A}_{i,k} = \langle \delta\epsilon_r \mathbf{E}_n^{(k)}, \mathbf{E}_n^{(i)} \rangle. \quad (2.18)$$

This eigenvalue problem generally can have  $N$  different solutions; the degenerate mode (with degeneracy  $N$ ), in general, splits into  $N$  different resonances owing to the structure perturbation.

### C. Example

The analysis presented in Subsections 2.A and 2.B applies to a general two-dimensional (2D) or three-dimensional photonic crystal structure. However, to demonstrate its efficacy, we concentrate on photonic crystals formed by 2D hexagonal arrays of dielectric posts, studied previously by the authors.<sup>6</sup> A defect is formed by deleting the post selected as the defect site, conveniently centered at the origin—see Fig. 1(b). The resulting microcavity possesses resonant frequency  $\omega_0$ . This resonance frequency can be tuned by slightly varying the radius of the deleted post  $i$ th's nearest neighbors [marked by arrows in Fig. 1(b)] from  $a$  to  $a + \delta a_i$ . Thus we use expression (2.12) with  $n = 0$  and with  $\delta\epsilon = (\epsilon_r - 1)\epsilon_0 \text{sgn}(\delta a)$  only within the thin annulus  $0 \leq \phi_i < 2\pi$ ,  $a \leq r_i \leq a + \delta a_i$  around each nearest neighbor. For small  $\delta a$ , it can be approximated as

$$\delta\omega_0 \approx \omega_0 (\eta_0 \|\mathbf{H}_0\|)^{-2} \pi a (\epsilon_r - 1) \sum_{i=1}^6 \delta a_i \overline{|E_0|_i^2}, \quad (2.19)$$

where  $\overline{|E_0|_i^2} \equiv (2\pi)^{-1} \int_0^{2\pi} |E_0(r_i = a)|^2 d\phi_i$  is the average of  $|E_0|^2$  along the  $i$ th post circumference. Note that in expression (2.19)  $\epsilon_r$  is constant. Expression (2.19) depicts a linear relationship between the resonance frequency variation  $\delta\omega_0$  and the post radii variations  $\delta a_i$ . A relation that links  $\delta\omega_0$  to small variations in post locations can be derived by a similar procedure.

As an example that demonstrates the accuracy of the above formulas, we use the cavity of Fig. 1(b), within the hexagonal structure studied previously by the authors.<sup>6</sup> The posts are made of a dielectric material with  $\epsilon_r = 8.41$ , radii of 0.6, and post spacing of 4 (arbitrary units). The resulting bandgap covers the range  $7.5 \leq \lambda \leq 10.5$  in arbitrary length units. The reference cavity obtained by a removal of a single post has a resonance wavelength  $\lambda_0 = 9.06$ . The corresponding electric field mode  $\mathbf{E}_0$  is shown in Fig. 1(c). We have used expression (2.19) to study the resonant wavelength  $\lambda_0$  when the radii of the six nearest posts are varied identically:  $\delta a_i = \delta a$ ,  $i = 1 \dots 6$  (see Fig. 2). In Fig. 3 the results are compared with the exact resonant wavelength obtained

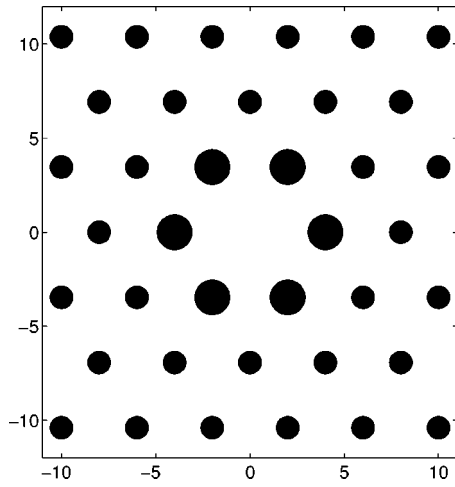
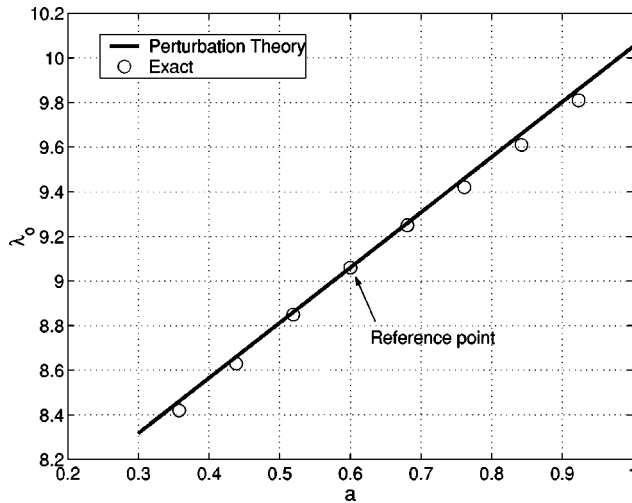


Fig. 2. Nearest neighbors radii variation.

Fig. 3. Resonance wavelength versus radii. The reference point is the point for which  $\delta\epsilon_r = 0$  and for which the mode  $E_0$  is computed.

by full-wave numerical computations.<sup>6</sup> It is seen that the results agree very well for a wide range of radii variations.

Finally, we note that the structure and its resonance can be adjusted to match the optical communication wavelength  $\lambda = 1.55 \mu\text{m}$  by scaling the structure by a factor of  $1.55 \mu\text{m}/9.06$ . The resulting post radius is  $0.103 \mu\text{m}$ , and the post distance is  $0.684 \mu\text{m}$ . The corresponding bandgap covers the range  $1.28 \mu\text{m} \leq \lambda \leq 1.8 \mu\text{m}$ .

### 3. RANDOM STRUCTURE INACCURACIES

Assume that an isolated defect is created within an otherwise perfect photonic crystal. The resulting microcavity, termed here the perfect microcavity, possesses the normalized modal field  $E_0$  and resonance frequency  $\omega_0$ . The resonant frequency of a microcavity located within an imperfect photonic crystal (i.e., a photonic crystal with structure inaccuracies such as random variations of the post radii) can now be obtained by applying the formulation of expressions (2.12) and (2.19) and Eqs. (2.13)–(2.18)

to the perfect microcavity structure and allowing  $\delta a$  to vary randomly from post to post. The result is identical to expression (2.19), except for the summation that is formally performed now over all posts in the crystal and where  $\delta a_i$  is the random change in the radius of the  $i$ th post. Since the modal field  $E_0$  of a perfect microcavity is well localized [see the example in Fig. 1(b)], it is clear that only the microcavity's closest neighbors contribute significantly to the above sum. Thus, for symmetric cavity and modes, one needs to include only  $N$  elements in the above sum ( $N = 6$  and  $N = 4$  for triangular and square lattices, respectively), where all have the same  $|E_0|^2_i$ . In this case, we obtain

$$\delta\omega_0 \approx \omega_0(\eta_0\|H_0\|)^{-2}\pi a(\epsilon_r - 1)\overline{|E_0|^2}\sum_{i=1}^N \delta a_i. \quad (3.1)$$

Note that all quantities in the right-hand side in expression (3.1) are deterministic except for the  $\delta a_i$ , which are zero-mean independent random variables. Therefore the average  $\langle\delta\omega_0\rangle$  vanishes, and the frequency-shift variance is given by (assuming  $\delta a_i$  has the same statistics for all  $i$ )

$$\begin{aligned} \langle(\delta\omega_0)^2\rangle &\approx [\omega_0(\eta_0\|H_0\|)^{-2}\pi a(\epsilon_r - 1)\overline{|E_0|^2}]^2 \\ &\times N\langle(\delta a)^2\rangle. \end{aligned} \quad (3.2)$$

Thus the variance increases with the number of closest neighbors  $N$  and with the average post radii  $a$ .

As an example, we have introduced random inaccuracies into the entire 2D structure depicted in Fig. 1 (see the numerical example in Section 2 for a detailed description of the structure). Each realization consists of independent random perturbations of all the post radii, uniformly distributed between  $\mp\delta a_{\text{max}}$  (i.e., in a single realization, different posts in the structure have different radii). The exact shift in the resonance wavelength was computed numerically for each realization, and its standard deviation was estimated on the basis of 40 realizations. This numerical experiment was repeated for five different values of  $\delta a_{\text{max}}$ , namely, 2%, 5%, 8%, 10%, and 12%. In Fig. 4 we compare the estimated standard deviation, (shown by circles) to that predicted by expression (3.2) using only

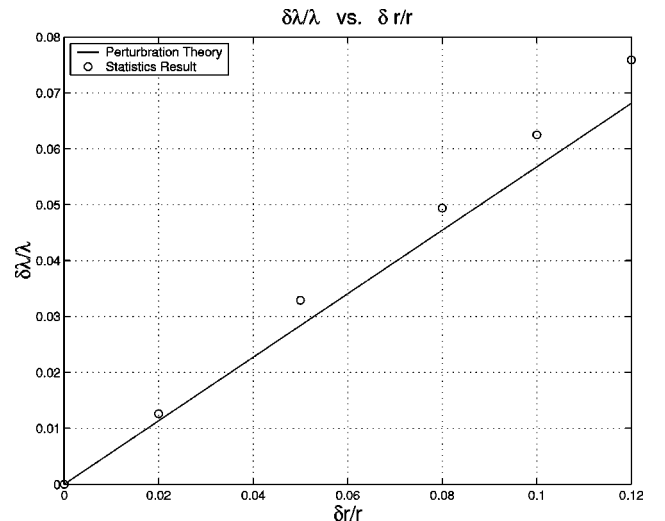


Fig. 4. Resonance wavelength standard deviation versus maximal magnitude of radii perturbations.

the six closest neighboring posts. It is seen that expression (3.2) provides a good qualitative estimate of the resonant wavelength deviation.

#### 4. COUPLED-CAVITY WAVEGUIDE

The procedure outlined in the previous sections can be used to build a model for a CCW in the presence of random structure inaccuracies. The mathematical model is based on the following physical observations:

1. The CCW microcavities are weakly coupled.

2. The lowest resonant frequency of the  $i$ th microcavity ( $i$  roam over all integers) is  $\omega_i = \omega_0 + \delta\omega_i$ , where  $\delta\omega_i$  is a random variable whose properties can be predicted by expressions (3.1) and (3.2) with  $\delta\omega_0 \mapsto \delta\omega_i$ .

3. Since, for sufficiently separated cavities,  $\omega_i$  depends essentially on the  $\epsilon$  variations of the  $i$ th microcavity's closest neighbors, the random variables  $\delta\omega_i$  are rendered independent.

Thus one can treat the entire waveguide as a linear array of weakly coupled independent cavities, each having a resonant frequency that slightly differs from  $\omega_0$ . According to the discussion in Section 2, the spatial form of the resonant mode is almost the same for each of the microcavities. Therefore our analysis is based essentially on the approach outlined in Ref. 6, with the modifications required to account for observations 1–3 above.

Let  $\epsilon_b(r)$  be the relative permittivity of the photonic crystal, including the random inaccuracies but excluding the defect sites. Thus  $\epsilon_b(r)$  describes a perfectly periodic photonic crystal, superimposed on which is some noisy structure that represents the random inaccuracy. Let  $\epsilon_{d_n}(r)$  and  $H_n(r)$  represent the aforementioned inaccurate crystal including the  $n$ th microcavity only and the associated mode, respectively. The corresponding resonant frequency is  $\omega_n$ . Note, that in the absence of random structure inaccuracy, we have  $\epsilon_{d_n}(r) = \epsilon_{d_0}(r - n\mathbf{b})$ , where  $\mathbf{b}$  is the intercavity spacing vector.<sup>6</sup> We define  $d_n$  as

$$d_n(r) = \frac{1}{\epsilon_{d_n}(r)} - \frac{1}{\epsilon_b(r)}, \quad (4.1)$$

which represents the single defect corresponding to the  $n$ th microcavity, in its true position. Note that owing to the random structure inaccuracies the shift-invariance property  $d_n(r) = d(r - n\mathbf{b})$  does not hold. Let  $\epsilon_r(r)$  be the relative permittivity of the entire photonic crystal structure, including the random inaccuracies and the linear array of defects that forms our CCW. We have

$$\frac{1}{\epsilon_r(r)} = \frac{1}{\epsilon_b(r)} + \sum_n d_n(r). \quad (4.2)$$

In accordance with Eq. (2.1a), we define the operators

$$\begin{aligned} \Theta &\equiv \nabla \times \frac{1}{\epsilon_r(r)} \nabla \times, & \Theta^b &\equiv \nabla \times \frac{1}{\epsilon_b(r)} \nabla \times, \\ \Theta_n &\equiv \nabla \times d_n(r) \nabla \times. \end{aligned} \quad (4.3)$$

The modal field of the  $n$ th microcavity when all other defects are absent,  $H_n(r)$ , satisfies

$$(\Theta^b + \Theta_n)H_n(r) = \left(\frac{\omega_n}{c}\right)^2 H_n(r), \quad (4.4)$$

where  $\omega_n$  is the resonant frequency of this microcavity [see item 2. above]. Likewise, the equation governing the field of the entire CCW structure can be written as

$$\Theta H(r) = \left(\Theta^b + \sum_n \Theta_n\right)H(r) = \left(\frac{\omega}{c}\right)^2 H(r). \quad (4.5)$$

Under the weak-coupling assumption, we can now express the total field  $H(r)$  as a sum over the modal fields of the isolated microcavities:

$$H(r) = \sum_m A_m H_m(r), \quad (4.6)$$

where  $A_m$  is a set of unknown coefficients. Here  $H_m$  satisfies Eq. (4.4), with  $n \mapsto m$ . By use of a variational formulation, the operating frequency  $\omega$  of the entire CCW structure, and the corresponding field  $H(r)$ , is the extremal point of the functional

$$\left(\frac{\omega}{c}\right)^2 = \frac{\langle H, \Theta H \rangle}{\langle H, H \rangle}. \quad (4.7)$$

With the expansion in Eq. (4.6), Eq. (4.7) gets the form

$$\left(\frac{\omega}{c}\right)^2 = \frac{\sum_m \sum_n A_n \overline{A_m} T_{nm}}{\sum_m \sum_n A_n A_m I_{nm}}, \quad (4.8)$$

where [by use of Eqs. (4.4) and (4.5)]

$$T_{nm} \equiv \langle H_n, \Theta H_m \rangle = \left(\frac{\omega_m}{c}\right)^2 I_{nm} + T'_{nm}, \quad (4.9a)$$

$$I_{nm} \equiv \langle H_n, H_m \rangle, \quad (4.9b)$$

$$T'_{nm} \equiv \left\langle H_n, \sum_{j \neq m} \Theta_j H_m \right\rangle. \quad (4.9c)$$

A difference equation that governs the  $A_n$ 's can now be obtained by finding the extremum of Eq. (4.8) with respect to the coefficients. This standard procedure has been applied in Ref. 6, and its derivation in the present case is completely identical. The result is the difference equation

$$\sum_n \left\{ \left[ \left(\frac{\omega_k}{c}\right)^2 - \left(\frac{\omega}{c}\right)^2 \right] I_{nk} + T'_{nk} \right\} A_n = 0, \quad \forall k. \quad (4.10)$$

This equation differs from the parallel one obtained in Ref. 6 in two aspects. First, here we have a  $k$  dependence of the leftmost frequency term (replace  $\omega_k$  with the deterministic microcavity resonance  $\omega_0$  to obtain the previous equation). Second, the double-indexed terms have formally lost their shift-invariance property. However, consistent with relation (2.10), the approximate equality for the modal shapes holds:

$$H_n(r) \approx H_0(r - n\mathbf{b}). \quad (4.11)$$

Specifically, the random structure inaccuracy affects essentially the local resonant frequencies  $\omega_k$  associated with each microcavity and has a negligible effect on the modal shapes. This effect is reduced even further by the inner products [Eqs. (4.9b) and (4.9c)] that average out small spatial perturbations. Thus we can approximate

$$\begin{array}{cccccccc} & \vdots \\ & \cdots & 0 & \tau_1 & \tau_0 + \Delta_{k-1} & \tau_1 & 0 & \cdots \\ \underline{\tau} + \underline{\Delta} = & & \cdots & 0 & \tau_1 & \tau_0 + \Delta_k & \tau_1 & 0 & \cdots \\ & & & \cdots & 0 & \tau_1 & \tau_0 + \Delta_{k+1} & \tau_1 & 0 & \cdots \\ & & & & \cdots & 0 & \tau_1 & \tau_0 + \Delta_{k+2} & \tau_1 & 0 & \cdots \\ & & & & \vdots \end{array} \quad (4.16)$$

$$I_{nk} \approx I_{0n-k} = \hat{I}_{n-k}, \quad (4.12a)$$

$$\hat{I}_m \equiv \langle H_0(r), H_0(r - m\mathbf{b}) \rangle, \quad (4.12b)$$

$$T'_{nk} \approx T'_{0n-k} = \tau_{n-k}, \quad (4.12c)$$

$$\tau_m \equiv \left\langle H_0(r - m\mathbf{b}), \sum_{j \neq 0} \Theta_j H_0(r) \right\rangle. \quad (4.12d)$$

Note that  $\hat{I}$  and  $\tau$  are obtained from Eqs. (4.9b) and (4.9c) by the mere replacement of  $H_m(r)$  with  $H_0(r - m\mathbf{b})$ , as stated in expression (4.11). To simplify further, we express the frequency  $\omega_k$  as

$$\omega_k = \omega_0 + \delta\omega_k, \quad \omega_k^2 \approx \omega_0^2 + 2\omega_0\delta\omega_k. \quad (4.13)$$

With these expressions, Eq. (4.10) becomes

$$\sum_n (\Omega^2 \hat{I}_{n-k} + 2c^{-2}\omega_0\delta\omega_k \hat{I}_{n-k} + \tau_{n-k}) A_n = 0, \quad \forall k, \quad (4.14)$$

where

$$\Omega^2 \equiv c^{-2}(\omega_0^2 - \omega^2). \quad (4.14a)$$

In the absence of structural noise, one has  $\delta\omega_k \equiv 0 \forall k$ . It is easily verified that in this case Eq. (4.14) reduces to the shift-invariant equation representing the perfect CCW case.<sup>6</sup> In the latter, we have exploited the perfect shift-invariance property to obtain a solution of the form  $A_n = \exp(i\beta n)$ , which subsequently leads to the dispersion equation (1.1)—after neglecting subdominant terms among the  $T'_{nm}$ . Here we find it beneficial to rewrite Eq. (4.14a) in the form of an infinite matrix eigenvalue problem. Note that, since the local modes decay exponentially away from the microcavities, their inner products [expression (4.12a)] decay exponentially with  $|n - k|$ . The dominant term among the  $\hat{I}_m$  is  $\hat{I}_0$ , which is nothing but the square of the  $H_0$  norm. Thus we can rewrite Eq. (4.14) in the matrix eigenvalue form

$$[\underline{\tau} + \underline{\Delta}]\mathbf{A} = -\Omega^2 \|H_0\|^2 \mathbf{A}, \quad (4.15)$$

where  $\mathbf{A}$  is a vector of the unknown coefficients  $A_n$ ,  $\underline{\Delta}$  is a diagonal matrix whose  $k$ th diagonal element is given by

$$\Delta_k = 2c^{-2} \|H_0\|^2 \omega_0 \delta\omega_k, \quad (4.15a)$$

and  $\underline{\tau}$  is a matrix whose  $m, n$ th entry is given by

$$\tau_{mn} = \tau_{m-n}. \quad (4.15b)$$

Note that  $\tau_k$ ,  $k \neq \pm 1$  is exponentially weak compared with  $\tau_{\pm 1}$  [ $\Theta_0$  is excluded in expression (4.12b)]. Furthermore, for symmetric modes we have  $\tau_m = \tau_{-m}$ . Thus the matrix in Eq. (4.15) is essentially of the form

Matrices of this structure appear widely in many areas of theory and applications. For a noiseless system,  $\Delta_k = 0$ , and the resulting form is sufficiently simple to allow analytic solution for its eigenvalues (see, for example, Ref. 10, Chap. 4). For a noiseless  $N \times N$  matrix we have

$$\Omega_n^2 |_{\delta\omega_k=0} = \|H_0\|^{-2} \{ \tau_0 - 2\tau_1 \cos[n\pi/(N+1)] \}, \quad (4.17)$$

$$n = 1 \dots N.$$

The perfect microcavity array waveguide corresponds to  $N \rightarrow \infty$ . In this case, the discrete set approaches a continuum, uniformly covering the interval

$$\|H_0\|^{-2} [\tau_0 - 2\tau_1, \tau_0 + 2\tau_1], \quad (4.18)$$

and this last result reconstructs the bandwidth prediction of Ref. 6:

$$\frac{\Delta\omega}{\omega_0} = 2 \left( \frac{c}{\omega_0 \|H_0\|} \right)^2 \tau_1. \quad (4.19)$$

The introduction of structural inaccuracy is manifested by the presence of  $\Delta_k \neq 0$  on the matrix diagonal. Since only the diagonal is affected, the structural noise results in random shifts of the corresponding eigenvalues:

$$\Omega_n^2 = \|H_0\|^{-2} \{ \tau_0 - 2\tau_1 \cos[n\pi/(N+1)] + \Delta_n \}, \quad (4.20)$$

$$n = 1 \dots N.$$

Evidently, these random shifts perturb the uniform covering of the interval in term (4.18). This perturbation becomes significant and opens holes in this interval only when  $\Delta_n$  approaches  $2\tau_1$  for some  $n$ . In other words, when [by use of Eqs. (4.15a) and (4.19)]

$$\delta\omega_n = O(\Delta\omega|_{\text{perfect waveguide}}) \quad \text{for some } n. \quad (4.21)$$

This result presents a qualitative, canonical, threshold condition for the structural noise level: If the structural inaccuracy variations render the deviation of the microcavities' resonance to exceed the bandwidth of the corresponding perfect CCW, the transmission properties of the perturbed CCW will degrade significantly. As long as the

structural inaccuracy renders  $\delta\omega_k$  below that threshold level, it is expected that the CCW properties will not degrade significantly.

To demonstrate the threshold effect, we have simulated the transmission of a CCW in a photonic crystal consist-

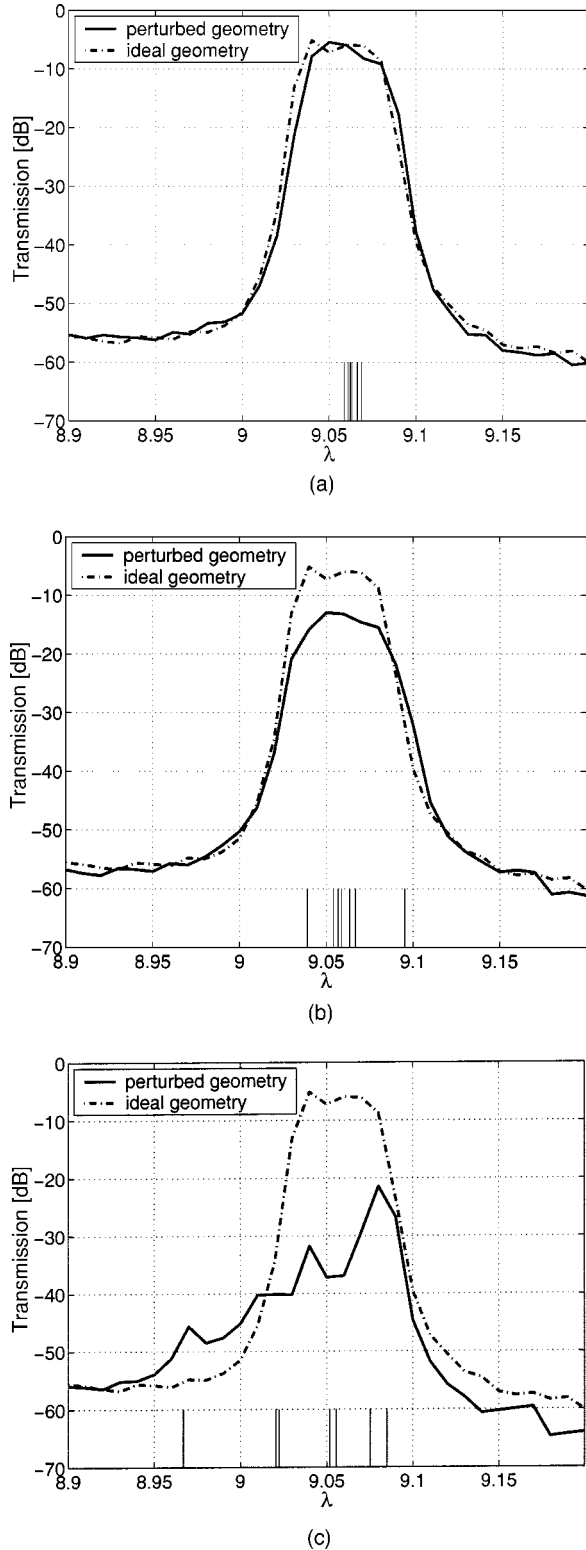


Fig. 5. Transmission of the perfect CCW (dashed-dotted curve) and the randomly perturbed CCW (solid curve) for post radii random inaccuracy of (a) 2%, (b) 5%, (c) 10%.

ing of a 2D hexagonal lattice of dielectric posts, whose parameters are identical to those used in the previous examples. The microcavities are obtained by a removal of a dielectric post, as shown in Fig. 1(b). The intercavity spacing is three periods in the horizontal direction, and the simulated CCW section consists of seven microcavities. The transmission of the perfect CCW is depicted in Fig. 5 by a dashed-dotted curve. In comparison, we show by a solid curve the transmission corresponding to the same CCW but with random radii perturbation, uniformly distributed between  $\mp\delta a_{\max}$ , with  $\delta a_{\max}/a = 2\%$ ,  $5\%$ , and  $10\%$ . The solid vertical lines show  $\delta\omega_k$ —the individual resonant wavelengths of each of the microcavities. It is seen that the CCW transmission degrades significantly if the variation exceeds the unperturbed CCW bandwidth, as predicted by the threshold relation in Eq. (4.21). We have performed several different realizations of this numerical experiment. All results were consistent with this prediction.

## 5. CONCLUSIONS

Cavity perturbation theory is used here as a mathematical model to estimate the performance degradation of microcavity filters and CCW devices under structure inaccuracies. For the microcavity, the theory predicts a frequency shift that is due to deterministic as well as random changes in the lattice structure and shows an approximate linear dependence between the variance of the structure parameters and that of the resonant frequency. The effect of structural noise on the CCW devices, however, is different in its nature: Random structure variations have practically no effect on the CCW performance if they are below the threshold level predicted by Eq. (4.21), and they may completely destroy the CCW behavior if this threshold level is exceeded. These theoretical results were verified by numerical computations. Our sensitivity analysis is important for applications in the optical and infrared regime, as the typical sizes of various components in the photonic crystal device may approach the limits of fabrication accuracy.

## APPENDIX A

Expand  $f_n$  in terms of the set  $\{g_m^\delta\}$ :

$$f_n = \sum_m a_m^n(\delta) g_m^\delta, \quad a_m^n(\delta) = \langle f_n, g_m^\delta \rangle. \quad (\text{A1})$$

Moving the  $n$ th term to the left and using orthogonality of the  $g_m^\delta$ , we get

$$\|f_n - a_n^n(\delta) g_n^\delta\|^2 = \sum_{m, m \neq n} |\langle f_n, g_m^\delta \rangle|^2. \quad (\text{A2})$$

Since  $\{g_m^\delta\}$  is a basis for any  $\delta$ , the sequence (in  $m$ )  $\{a_m^n(\delta)\}$  is square summable. Also, by hypothesis  $\sum_{m, m \neq n} |\langle f_n, g_m^\delta \rangle|^2 \rightarrow 0$  as  $\delta \rightarrow 0$ . Therefore the sum in the right-hand side of Eq. (A2) above must vanish with  $\delta$ . In other words,

$$\|f_n - a_n^n(\delta) g_n^\delta\| \rightarrow 0 \quad \text{as } \delta \rightarrow 0. \quad (\text{A3})$$

In the case that the sum on the right-hand side of Eq. (A2) is bounded by  $O(\delta)$ , the same bound holds for the left-hand side of expression (A3),

$$\|f_n - a_n^n(\delta)g_n^\delta\| \leq O(\delta) \quad \text{as } \delta \rightarrow 0, \quad (\text{A4})$$

which proves the theorem.  $\square$

B. Z. Steinberg can be reached by e-mail at steinber@eng.tau.ac.il, and A. Boag can be reached by e-mail at boag@eng.tau.ac.il.

## REFERENCES

1. E. Centeno, B. Guizal, and D. Felbacq, "Multiplexing and demultiplexing with photonic crystals," *J. Opt. A Pure Appl. Opt.* **1**, L10–L13 (1999).
2. N. Stefanou and A. Modinos, "Impurity bands in photonic insulators," *Phys. Rev. B* **57**, 12127–12133 (1998).
3. M. Bayindir, B. Temelkuran, and E. Ozbay, "Tight-binding description of the coupled defect modes in three-dimensional photonic crystals," *Phys. Rev. B* **61**, 11855–11858 (2000).
4. A. Yariv, Y. Xu, R. K. Lee, and A. Scherer, "Coupled-resonator optical waveguide: a proposal and analysis," *Opt. Lett.* **24**, 711–713 (1999).
5. A. Boag, M. Gafni, and B. Z. Steinberg, "Bandwidth control for photonic bandgap waveguides," in *Proceedings of Bi-anisotropics 2000, the Eighth International Conference on Electromagnetics of Complex Media* (Instituto Superior Tecnico, Lisbon, 2000), pp. 321–324.
6. A. Boag and B. Z. Steinberg, "Narrow-band microcavity waveguides in photonic crystals," *J. Opt. Soc. Am. A* **18**, 2799–2805 (2001).
7. R. E. Peierls, *Quantum Theory of Solids* (Oxford Clarendon Press, Oxford, UK, 1955).
8. R. F. Harrington, *Time Harmonic Electromagnetic Fields* (McGraw Hill, New York, 1961).
9. J. D. Joannopoulos, R. D. Meade, and J. N. Winn, *Photonic Crystals: Molding the Flow of Light* (Princeton U. Press, Princeton, N. J. 1995).
10. P. Lancaster and M. Tismenetsky, *The Theory of Matrices*, 2nd ed. (Academic, Orlando, Fla., 1985).